

# Preparation of cotton linter nanowhiskers by high-pressure homogenization process and its application in thermoplastic starch

N. R. Savadekar · V. S. Karande · N. Vigneshwaran ·  
P. G. Kadam · S. T. Mhaske

Received: 9 April 2014 / Accepted: 29 April 2014 / Published online: 1 June 2014  
© The Author(s) 2014. This article is published with open access at Springerlink.com

**Abstract** The present work deals with the preparation of cotton linter nanowhiskers (CLNW) by acid hydrolysis and subsequent processing in a high-pressure homogenizer. Prepared CLNW were then used as a reinforcing material in thermoplastic starch (TPS), with an aim to improve its performance properties. Concentration of CLNW was varied as 0, 1, 2, 3, 4 and 5 wt% in TPS. TPS/CLNW nanocomposite films were prepared by solution-casting process. The nanocomposite films were characterized by tensile, differential scanning calorimetry, scanning electron microscopy (SEM), water vapor permeability (WVP), oxygen permeability (OP), X-ray diffraction and light transmittance properties. 3 wt% CLNW-loaded TPS nanocomposite films demonstrated 88 % improvement in the tensile strength as compared to the pristine TPS polymer film; whereas, WVP and OP decreased by 90 and 92 %, respectively, which is highly appreciable compared to the quantity of CLNW added. DSC thermograms of nanocomposite films did not show any significant effect on melting temperature as compared to the pristine TPS. Light transmittance ( $T_t$ ) value of TPS decreased with increased content of CLNW. Better interaction between CLNW and TPS, caused due to the hydrophilic nature of both the materials, and uniform distribution of CLNW in TPS were

the prime reason for the improvement in properties observed at 3 wt% loading of CLNW in TPS. However, CLNW was seen to have formed agglomerates at higher concentration as determined from SEM analysis. These nanocomposite films can have potential use in food and pharmaceutical packaging applications.

**Keywords** Cotton linter · Starch · Water vapor permeability · Oxygen permeability · Differential scanning calorimetry

## Introduction

Cellulose micro/nanoparticle-reinforced polymer composites are a fast growing area of research because of their enhanced mechanical, barrier, and biodegradation properties. This rapidly expanding field is generating many exciting new materials with novel properties. Among the many kinds of candidates of biodegradable polymer, starch is one of the most promising materials as it is a versatile biopolymer with immense potential and low price for use in the non-food industries (Choi et al. 1999). The nanocomposite materials display a significant improvement in the mechanical properties even at very low reinforcement content (Angles and Dufresne 2000). Compared with inorganic fillers, the major advantages of the fillers from renewable resources such as cellulose (Cao et al. 2007; Nishino et al. 2004), starch, (Angellier et al. 2006) and chitin (Gopalan and Dufresne 2003) are their sustainability, availability, low cost, low energy consumption and high-specific mechanical performance (Azizi Samir et al. 2005). Starch is a widely available, renewable, low cost, and biodegradable biopolymer. For these reasons, starch generates a great interest and is considered as a promising

N. R. Savadekar · V. S. Karande · P. G. Kadam ·  
S. T. Mhaske (✉)  
Department of Polymer and Surface Engineering Technology,  
Institute of Chemical Technology, Matunga (E), Mumbai  
400019, Maharashtra, India  
e-mail: stmhaske@gmail.com

N. Vigneshwaran  
Nanotechnology Research Group, Central Institute for Research  
on Cotton Technology, Matunga, Mumbai 400019, Maharashtra,  
India

alternative to synthetic polymers for packaging applications.

By incorporating plasticizing agent such as water and/or polyhydric alcohols, starch can be made thermoplastic and called thermoplastic starch (TPS) or plasticized starch (PS) through its de-structurization by the introduction of mechanical and heat energy. Thermoplastic starch (TPS) alone often cannot meet the mechanical and barrier properties, for commercial and technical requirements. (Carvalho et al. 2003; Gaudin et al. 2000) TPS has attracted considerable attention during the past two decades and offered an interesting alternative for synthetic polymers where long-term durability is not needed and rapid degradation is an advantage (Van Soest et al. 1996).

Currently, the materials used in packaging industries are produced from fossil fuels and are practically non-degradable. Materials used for foodstuff packaging, having short-term usage, represent a serious environmental problem. Efforts to extend their shelf life and enhance food quality, while reducing packaging waste has encouraged the exploration of new bio-based packaging materials such as edible and biodegradable films from renewable resources (Sorrentino et al. 2007).

Nanocellulose, i.e., nanocrystals or nanofibers have been used to reinforce starch and improve its performance properties (Angles and Dufresne 2000, 2001; Kvien et al. 2007; Savadekar and Mhaske 2012). It is well known that native cellulose, when subjected to strong acid hydrolysis can be readily converted to microcrystalline cellulose (Chazeau et al. 2000; Beck-Candanedo et al. 2005; Bondeson et al. 2006; Zhang et al. 2007). However, preparation of cellulose-based nanowhiskers and its application as a reinforcing material in bio-polymers is a relatively new field within nanotechnology that has generated considerable interest in the last decade, especially within the biopolymer community. Solution casting is the most common method used for preparing cellulose-based nanocomposites (Dufresne et al. 1999; Grunert and Winter 2002; Kvien and Oksman 2007; Petersson et al. 2007; Pu et al. 2007).

Many researchers worked on biodegradable polymeric matrices such as starch (Savadekar et al. 2013; Choi and Simonsen 2006; Lu et al. 2006), soy protein (Lu et al. 2004), silk fibroin (Wongpanit et al. 2007), polylactide (PLA) (Huang et al. 2006), or poly(vinyl alcohol) (PVA) (Zhang et al. 2007) and non-biodegradable polymeric matrices such as polypropylene (Ljungberg et al. 2005), poly(vinyl chloride) (Chazeau et al. 2000), poly(oxyethylene) (Azizi Samir et al. 2005) and epoxy resin (Shimazaki et al. 2007) have been utilized in making nanocomposites containing cellulose nanowhiskers, nanocrystals, or nanofibers as reinforcing agent and improvements were observed in their mechanical and functional properties.

Raw cotton linters are a waste product comprising a mixture of residual cotton lint and cotton linters left on the cottonseed after ginning. These fibers are leftover as they are too short for normal uses. The raw cotton linters contain residual waxes and oils in the natural state, which make the fibers quite hydrophobic, and they are generally used as a low-cost stock feed. The annual world production of cotton linter is estimated to be 18 million tons in 2001, supposedly the third largest fiber source after wood and bamboo (Eichhorn et al. 2010). Utilizing natural fillers from renewable resources not only contributes to a healthy ecosystem, but also makes them economically interesting for industrial applications due to the high performance of the resulting composites (Lu et al. 2004).

In this work, we first prepared microcrystalline cellulose (MCC) from cotton linter by the process of acid hydrolysis. Prepared MCC was then subjected to processing in a high-pressure homogenizer to prepare cotton linter nanowhiskers (CLNW). The resulting CLNW were used as a reinforcing agent in thermoplastic starch (TPS) to prepare its nanocomposite films, with an aim to improve its performance properties. TPS/CLNW nanocomposite films were characterized for tensile, thermal, morphological, light transmittance, water vapor permeability and oxygen permeability properties. Substantial improvement in the tensile, water vapor permeability and oxygen permeability properties were expected, mainly due to the hydrophilic nature of both TPS and CLNW, suggesting better interaction between them.

## Experimental

### Materials

Cotton linter nanowhiskers were prepared from cotton linters in the lab by acid hydrolysis and subsequent processing in a high-pressure homogenizer. Cotton linters were supplied by Balaji Cotton Linter Pvt. Ltd., Gujarat, India. Thermoplastic starch (TPS), glycerol and hydrochloric acid were supplied by S. D. Fine Chem Pvt. Ltd., Mumbai, India. Glacial acetic acid (99 % purity) was obtained from Merck Specialities Pvt. Ltd., Mumbai, India. All chemicals were used as obtained without any modification or purification.

### Preparation of cotton linter nanowhiskers (CLNW)

Cotton linters were first hydrolyzed using 4 N HCl (1:5 weight ratio) in an autoclave for 30 min at a pressure of 103,421.4 Pa and temperature of 50 °C to get MCC. The obtained MCC was neutralized by washing it several times

with distilled water. After neutralization, MCC was filtered through 200-mesh size cloth and dried in vacuum oven at 50 °C for 24 h. Dried MCC was sieved through 105 micron and 53 micron size sieves. MCC was then dispersed in 1,000-ml distilled water to prepare 1 % (w/w) solution of it using a stirrer maintained at 1,500 rpm for 2 h. MCC solution was then homogenized using a high-pressure homogenizer (241 MPa) to convert it into CLNW. MCC solution was passed repeatedly 15 times through the high-pressure homogenizer to get CLNW, as per the procedure described by Karande et al. (Karande et al. 2013). CLNW prepared by this process were characterized using SEM analysis; and further used as a reinforcing agent in TPS. From SEM analysis (Fig. 8a), it can be clearly observed that the prepared CLNW had diameter in the range of 50–100 nm.

#### Preparation of TPS/CLNW nanocomposite films

The preparation of TPS/CLNW nanocomposite films was based on solution-casting process. CLNW in various concentrations (1, 2, 3, 4 and 5 % w/w of TPS) was dispersed in 100-ml distilled water under continuous stirring at 1,000 rpm for 15 min. Then, TPS (5 g) was added into the CLNW solution until the complete dissolution of TPS, which took around 6 h. Glycerol content (plasticizer), based on TPS, was fixed at 30 wt%; while acetic acid (anti-microbial agent) at 20 wt%. TPS/CLNW solution added with glycerol and acetic acid were mixed at 1,000 rpm when simultaneously heated at 70 °C for 30 min, until the mixture was gelatinized. The solution was then poured in acrylic mold (dimension 20 × 18 × 2 cm) and kept in an air circulating oven at 50 °C for 24 h to dry. Formed films were removed smoothly from the molds and stored in a desiccator maintained at 25 °C and RH of 70 %. Pristine TPS film was also prepared using the same procedure, but, without any addition of CLNW into it. Average film thickness of the films was determined to be 60 ± 5 μm using a thickness gauge.

### Characterizations and testing

#### Tensile properties

Tensile properties such as tensile strength and percent strain at break of the pristine TPS and TPS/CLNW nanocomposite films were determined using a Universal Testing Machine (LR-50 K, LLOYD instrument, UK) using a 500 N load cell, in accordance to ASTM D 882 and crosshead speed of 50 mm/min. An average value of six replications for each sample was taken.

#### Differential scanning calorimetry (DSC)

DSC was used to measure the thermal transitions of TPS and TPS/CLNW nanocomposite films. The test was performed with a Q100 DSC (TA Instruments) differential scanning calorimeter equipment, fitted with a nitrogen-based cooling system. All the measurements were performed in the temperature range of –50 to 150 °C at a heating rate of 10 °C/min.

#### X-ray diffraction (XRD) analysis

XRD analysis of the prepared films was performed using a Rigaku miniflex X-ray diffractometer equipped with a Cu target having wavelength of 1.54 Å. The samples were scanned in the angular range from 2 to 40° at a scanning rate of 2°/min.

#### Water vapor permeability (WVP)

WVP values of the films were determined gravimetrically as per the ASTM standard of E96 (water method). Each test film was sealed on the top of permeation cell containing distilled water using melted paraffin. The permeation cells were placed in desiccator maintained at 0 % RH using anhydrous calcium chloride. The water transferred through the film and absorbed by the desiccant was determined from the weight of the permeation cell. Each permeation cell was weighed at an interval of 24 h. The WVP was expressed in g/m s Pa. An average value of three replicates for each sample was taken.

#### Oxygen permeability (OP)

OP of the films was determined using an oxygen permeability test machine (Labthink BTY-B1). The film was placed in a cell and oxygen was introduced on one side of the film. Chamber humidity was maintained at 50 % and temperature at 30 °C. OP was expressed in cm<sup>3</sup> cm/cm<sup>2</sup> s cm Hg. An average value of three replicates for each sample was taken.

#### Light transmittance

The light transmittance (Tr) of the TPS and TPS/CLNW films was measured using an ultraviolet–visible (UV–Vis) spectroscope (UV-160A, Shimadzu, Japan) at a wavelength range of 200–800 nm.

#### Scanning electron microscopy (SEM)

SEM analysis was carried out with a JEOL<sup>®</sup> 6380 LA (Japan) scanning electron microscope. Nanocomposite samples

were fractured under liquid nitrogen to avoid any disturbance to the molecular structure and then were coated with gold before imaging; whereas, the dried samples of CLNW were observed directly after coating with gold. Samples were observed with an accelerating voltage of 15 kV.

## Results and discussion

### Tensile properties

The values of tensile strength obtained for TPS and TPS/CLNW nanocomposite films are depicted in Fig. 1. TPS was found to have tensile strength of about 9 MPa. Values of tensile strength of TPS increased with increased addition of CLNW in it. However, this increase in the values of tensile strength of TPS was observed up to a 3 wt% addition of CLNW. Tensile strength was determined to have shown an improvement of 88 % for 3 wt% CLNW-added TPS nanocomposite films. This increase in the value of tensile strength for TPS is highly appreciable compared to the amount of CLNW added. Increase in tensile strength up to 3 wt% addition of CLNW in TPS is attributed to the better interactions happening between TPS and CLNW, due to the hydrophilic nature of both the materials. Moreover, uniform and individual level distribution of CLNW in TPS up to 3 wt% (as observed from scanning electron microscopy described ahead) concentration brought about maximum possible availability of surface area of CLNW to interact with TPS. These interactions led to a better alignment of TPS molecules with CLNW nanoparticles, increasing the crystallinity (this has been confirmed by the X-ray diffraction analysis ahead). Thus, it can be said that CLNW induced nucleating effect in TPS, increasing its crystallinity and thus the tensile properties up to a particular concentration. Savadekar and Mhaske (2012) have quoted similar reason for the nanocellulose fiber-reinforced TPS-based nanocomposite films. This better interaction has also been a cause for the improvement of properties observed for nanosilica-reinforced k-carrageenan bio-composite films (Rane et al. 2014). While Savadekar et al. (2013) also demonstrated an improvement of 18 % for 3 wt% nanoalumina-added poly(butylene adipate-co-terephthalate) composite films. The tensile strength values obtained for 4 and 5 wt% CLNW-loaded TPS nanocomposite films were lower than those of the other nanocomposite films. However, the value obtained for 4 wt% CLNW-added TPS nanocomposite film was still higher than that of pristine TPS film. CLNW, when loaded at 4 and 5 wt% concentration in TPS, started form aggregates (as demonstrated in Fig. 8 by SEM analysis). This aggregate formation by CLNW decreased its effective surface area to interact with CLNW and generated

point of stress concentrate, decreasing the level of interactions between CLNW and TPS, decreasing crystallinity and thus the nucleating effect induced.

The percentage strain at break values obtained for the TPS and TPS/CLNW nanocomposite films is depicted in Fig. 2. Values of percentage strain at break decreased with increased concentration of CLNW in TPS; however, the decrease in the values of percentage strain at break is less as compared to the increase observed in the values of tensile strength. This was attributed to the increased stiffness of the nanocomposite films as compared to the pristine TPS films, caused due to better interaction happening between the two which ultimately led to increase in the crystallinity of the nanocomposite films. This decreased the ability of the TPS polymer chains to move past each other decreasing the elongation property. Here too, the values of percentage strain at break decreased up to 3 wt% concentration of CLNW in TPS; whereas, increased for higher concentration, which must have caused due to the formation of aggregates of CLNW at higher concentration, decreasing the effective surface area for interacting with TPS, decreasing the stiffness as well and subsequently increasing the percentage strain. Aggregates formed decreased the crystallinity of TPS due to the decrease in the effective surface area of CLNW to interact with TPS.

Thus, it can be said that 3 wt% CLNW-loaded TPS nanocomposite films demonstrated optimum improvement in the tensile properties, which is further confirmed through the morphological, WVP, OP and crystallinity analysis.

### Differential scanning calorimetry (DSC)

The DSC thermograms obtained for the TPS and TPS/CLNW nanocomposite film samples are depicted in Fig. 3, which is a plot of heat flow (W/g) vs. temperature (°C). The DSC thermograms of pristine TPS and the nanocomposite films showed transitions occurring over a quite broad temperature range.

The TPS/CLNW nanocomposite films demonstrated a little insignificant effect on the melting (enthalpy of melting) characteristics as compared to the pristine TPS films (120.59 °C). However, by the addition of CLNW the melting temperature of pure TPS slightly shifted to higher temperature (122.94 °C for 3 wt% CLNW-loaded TPS nanocomposite films), which was attributed to better interactions happening between TPS and CLNW and uniform distribution of CLNW in TPS. While only minor increase was determined in the values of melting temperature when TPS was added with higher content of CLNW (i.e., 4 and 5 wt%) due to the formation of CLNW agglomerates as determined through SEM analysis. Sanchez-Garcia and Lagaron (2010) reported similar effect for addition of nanofiber of cellulose (NFC) on the thermal property of polylactic acid.

**Fig. 1** Influence of CLNW loading on tensile strength of TPS nanocomposite films

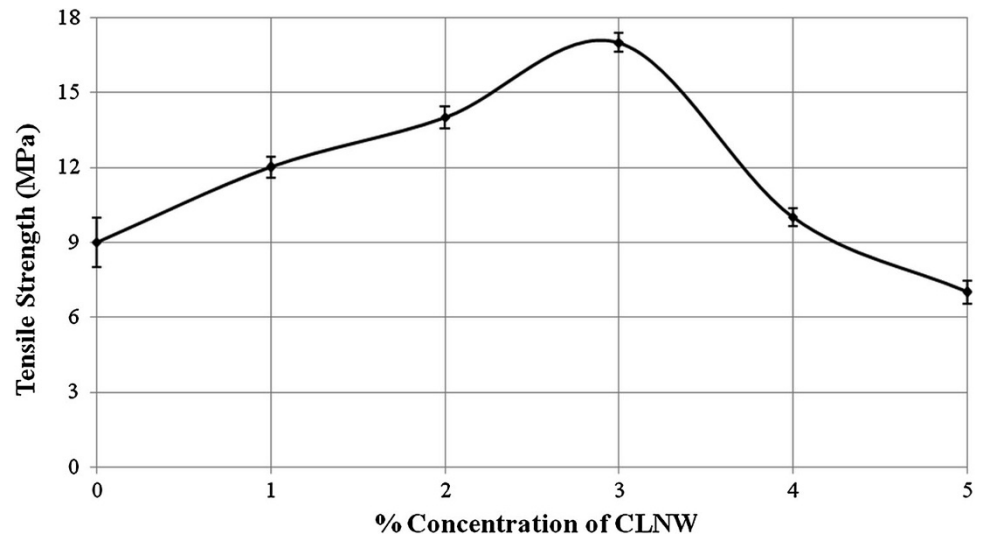
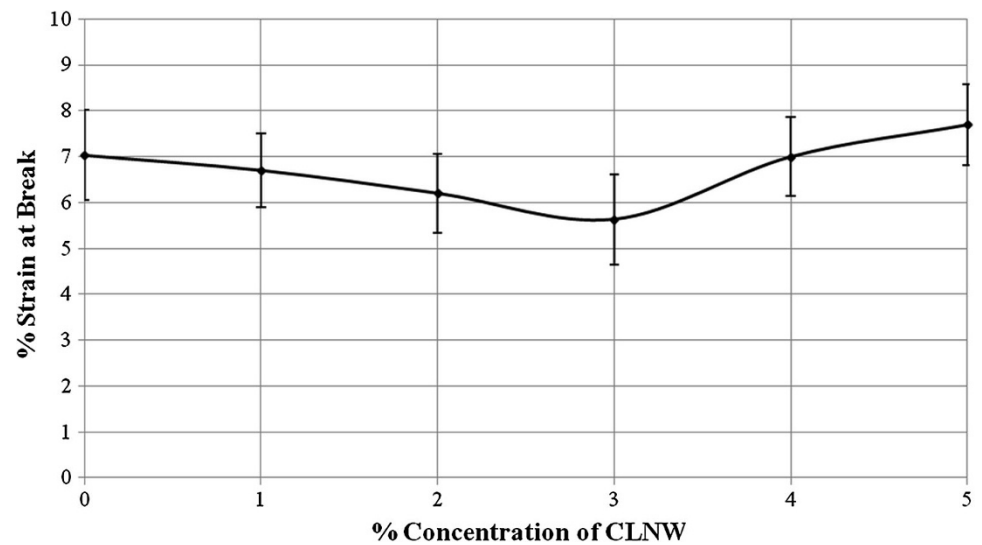


**Fig. 2** Influence of CLNW loading on percentage elongation at break of TPS nanocomposite films



#### X-ray diffraction (XRD) analysis

The X-ray diffraction (XRD) patterns recorded for CLNW, pristine TPS and TPS/CLNW nanocomposite films are illustrated in Fig. 4. The CLNW diffractogram displayed well-defined peaks, typical of a highly crystalline structure. The peak at  $2\theta = 14.7^\circ$ ,  $2\theta = 16.3^\circ$ ,  $2\theta = 22.6^\circ$ , and  $2\theta = 34.7^\circ$  corresponded to its (101), (101), (002), and (040) crystallographic planes, respectively, which were characteristic of cellulose type I. CLNW are crystalline materials. Crystalline regions increased the rigidity of CLNW.

The nanocomposite film samples displayed a diffraction peak around  $2\theta = 16.3^\circ$  and  $2\theta = 22.6^\circ$ , which correspond to the XRD pattern of cellulose-I-type crystalline structure. Intensity of this peaks increased with increased concentration of CLNW in TPS, suggesting its presence in their particular concentration levels, also suggesting increased crystallinity, induced due to better interaction happening

between TPS and CLNW, most probably due to the hydrophilic nature of both the materials. As described later, the expected properties of the composite materials could be enhanced using these CLNW with higher rigidity as reinforcing agent in the TPS polymer matrix.

#### Water vapor permeability (WVP)

The values of WVP obtained for the TPS and TPS/CLNW nanocomposite films are shown in Fig. 5. TPS is an hydrophilic polymer, and hence it has high WVP of about  $4.68 \times 10^{-9}$ /gm s Pa. Values of WVP decreased appreciably on addition of CLNW into the TPS films. The presence of dispersed phase of the rigid CLNW in TPS increased the tortuosity of the films, increasing the travel path of the water molecules to get through the nanocomposite films; thus, decreasing the intensity of water transmittance from the film. In addition, the interactions



**Fig. 3** DSC thermograms obtained for the prepared TPS and TPS/CLNW nanocomposite films

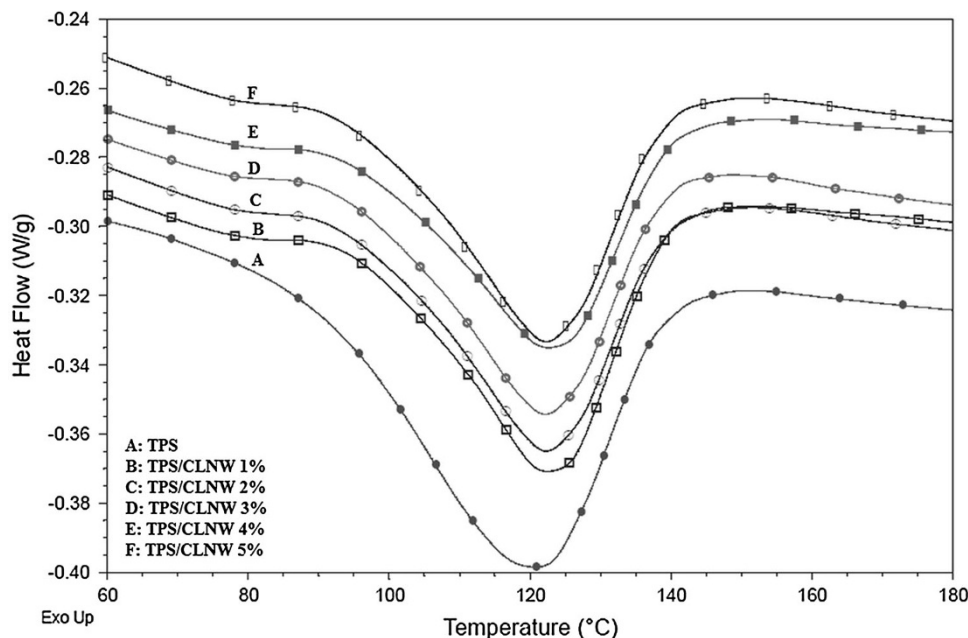
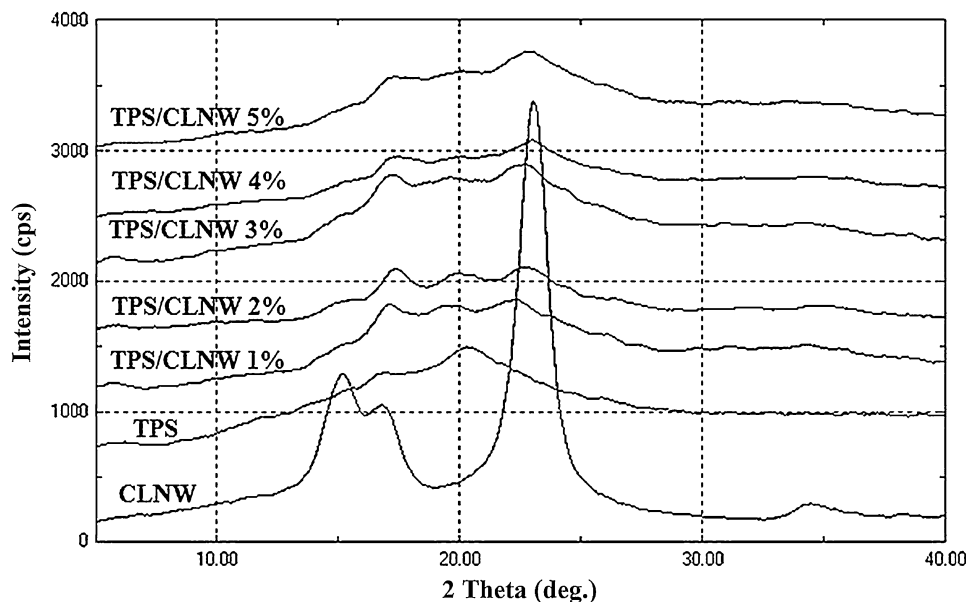


**Fig. 4** X-ray diffractograms obtained for CLNW, TPS and TPS/CLNW nanocomposite films



happening between CLNW and TPS increased the level of crystallinity in the nanocomposite films, further bringing about increase in the tortuosity in the films. Significant decrease in WVP value ( $2.5 \times 10^{-10}$  g/m s Pa) from an initial value of  $4.68 \times 10^{-9}$  g/m s Pa was recorded for 3 wt% CLNW-loaded TPS nanocomposite films, which is a decrease of about 90 % and is remarkable compared to the amount of CLNW added in TPS to prepare the nanocomposite films. Further increase in the content of CLNW slightly increased the value of WVP; however, those were still lower than that obtained for the pristine TPS. Formation of aggregates by CLNW (determined from SEM analysis mentioned ahead) decreased the effective surface

area for interaction between CLNW and TPS, decreasing the crystallinity and thus the level of tortuosity of the path for water molecules to travel. In addition, the decrease in the effective surface area of CLNW due to the formed aggregates was not able to physically resist the water transmittance as effectively as that possible with the individually dispersed CLNW at lower concentrations. Trend observed in the values of WVP with increased concentration of CLNW is in correlation with that of tensile properties. Thus, even though both TPS and CLNW are hydrophilic materials, the WVP of TPS decreased with increased addition of CLNW mainly due to the crystallinity induced by it into the TPS matrix.

**Fig. 5** Influence of CLNW loading on the WVP property of TPS nanocomposite films

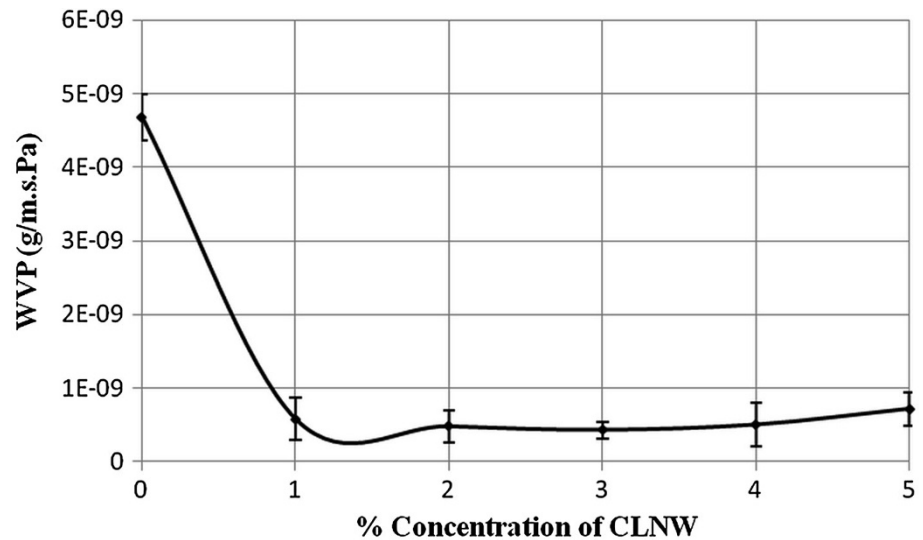
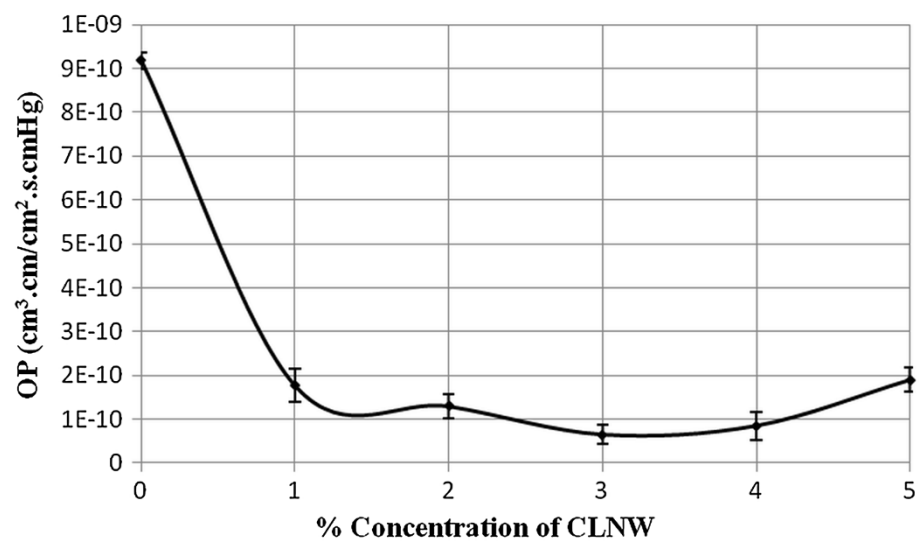


**Fig. 6** Influence of CLNW loading on the OP property of TPS nanocomposite films



#### Oxygen permeability (OP)

Figure 6 shows the plot of OP obtained for the TPS and its nanocomposite films against the concentration of CLNW. TPS was found to have OP of about  $9.3 \times 10^{-10} \text{ cm}^3 \text{ cm/cm}^2 \text{ s cm Hg}$ . However, the values of OP for TPS decreased with increased concentration of CLNW in it. As illustrated in Fig. 6, the maximum reduction of OP (i.e., 92 %) compared to pristine TPS was obtained for 3 wt% CLNW-loaded TPS nanocomposite films, which is a very appreciable decrease compared to the amount of CLNW added. This is attributed to the generation of tortuous path by the increased crystallinity induced by CLNW in TPS due to the interactions happening between them and to the physical presence of rigid CLNW nanoparticles, decreasing the permeation of oxygen molecules through the nanocomposite film. Values of OP increased slightly for TPS nanocomposite films added with CLNW concentrations of

4 and 5 wt%, but the values were still lower than that of pristine TPS films. Excess of CLNW (4 and 5 wt%) addition in TPS was a likely cause of phase separation, poor particle filler distribution and agglomerates formation which led to decrease in crystallinity of TPS nanocomposite films increasing the values of OP values as compared to 3 wt% CLNW-loaded TPS nanocomposite films.

Thus, 3 wt% addition of CLNW in TPS brings about optimized decrease ( $\geq 90$  %) in the WVP and OP properties of TPS.

#### Light transmittance

The light transmittance ( $T_r$ ) of the TPS and TPS/CLNW nanocomposite films, in the wavelength range of 200–800 nm, is shown in Fig. 7.  $T_r$  values of TPS decreased with increased concentration of CLNW. The  $T_r$  value at 800 nm reflects the transparency of the films,

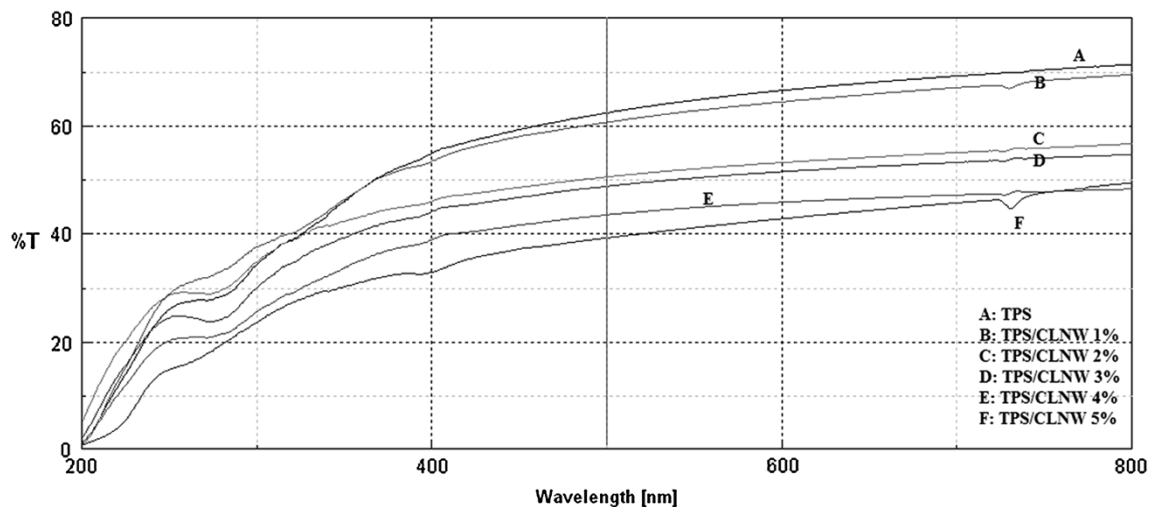


**Fig. 7** Influence of CLNW loading on light transmittance property of TPS nanocomposite films

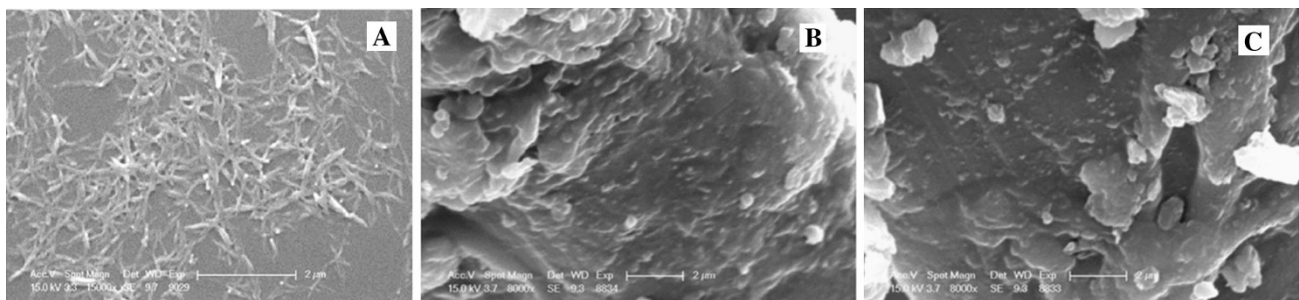


**Fig. 8** SEM images obtained for CLNW (a), 3 wt% CLNW-loaded TPS (b) and 4 wt% CLNW-loaded TPS (c)

which also provides some information on the particle size and degree of dispersion of the fillers within the matrix. For example, at a wavelength of 800 nm, the  $T_r$  values of TPS/CLNW 1 wt% and pristine TPS were 70 and 72 %, respectively. However, in the case of 2 and 3 wt% CLNW-loaded TPS nanocomposite films, the  $T_r$  values got decreased to 58 and 56 %, respectively, which is a drastic decrease. This is again attributed to the presence of rigid CLNW nanoparticles as well as the nucleating effect induced by CLNW in the TPS polymer matrix phase.

#### Scanning electron microscopy (SEM)

Figure 8 shows the SEM images obtained for CLNW nanoparticles (a), 3 wt% CLNW-loaded TPS nanocomposite films (b) and 4 wt% CLNW-loaded nanocomposite films (c).

From Fig. 8a, it can be seen that the average diameter of the nanowhiskers prepared from cotton linters through acid hydrolysis and subsequent processing in a high-pressure homogenizer was in the range of 50–100 nm. It can also be seen that all the nanowhiskers had uniformity in their size

and shape, which is as suggested by Karande et al. (2013) for the 15-time passed samples from the homogenizer.

The examination of the fractured surface of TPS/CLNW composites was carried out using a scanning electron microscope. Figure 8b, c shows the SEM micrographs of the samples, which were fractured under liquid nitrogen for 3 and 4 wt% CLNW-loaded TPS nanocomposite films, respectively.

As evident from the Fig. 8b, dispersion of CLNW in TPS matrix was uniform at 3 wt% concentration and above which started forming agglomerates as can be seen in Fig. 8c. Formation of agglomerates in 4 wt% CLNW-loaded TPS might have resulted in poor interfacial adhesion between CLNW and TPS matrix. Due to this at higher concentration CLNW, i.e., above 3 wt%, overall reduction in the tensile, WVP and OP properties might have been observed. The SEM micrographs Fig. 8b (TPS/CLNW 3 wt%) also provide an evidence of the strong interfacial adhesion between the CLNW and the TPS matrix and good dispersion of CLNW within the TPS matrix, without noticeable aggregates. Due to this good dispersion, tensile strength must have been improved by 88 % and drop in



WVP and OP was observed. Obviously, in the case of 4 wt% CLNW-filled TPS (Fig. 8c), poor interfacial adhesion between the CLNW and the TPS matrix, poor particle distribution and larger agglomerates formation led to mechanical and barrier properties to deteriorate.

## Conclusion

Cotton linter nanowhiskers (CLNW) were successfully prepared by the acid hydrolysis and subsequent processing in high-pressure homogenizer. Obtained CLNW were utilized as reinforcing agent in TPS polymer matrix, by incorporating it in various concentrations as 0, 1, 2, 3, 4 and 5 wt%. Prepared nanocomposite films were examined for tensile, thermal, morphological, water vapor permeability, oxygen permeability, light transmittance and X-ray diffraction properties. The nanocomposite films exhibited excellent tensile properties, lower water vapor permeability and oxygen permeability in comparison to the neat TPS film. Tensile strength increased with increasing the CLNW concentration up to 3 wt%, but after that the tensile strength decreased. The SEM images demonstrated uniform distribution of CLNW in the TPS matrix up to 3 wt% concentration, and agglomerates were witnessed at higher concentrations. CLNW-added TPS nanocomposite films displayed a shift towards high-temperature side of the melting endotherm. Transmittance of nanocomposite films decreased with increasing CLNW. These obtained properties were attributed to better interaction between CNLW and TPS caused due to the hydrophilic nature of both the materials.

**Acknowledgments** The authors are thankful to National Agricultural Innovation Project (NAIP), Indian Council of Agricultural Research (ICAR) for the keeping support through its Sub-project entitled ‘Synthesis and characterization of CNW and its application in biodegradable polymer composites to enhance their performance’, code number ‘C2041’.

**Open Access** This article is distributed under the terms of the Creative Commons Attribution License which permits any use, distribution, and reproduction in any medium, provided the original author(s) and the source are credited.

## References

- Angellier H, Molina-Boisseau S, Dole P, Dufresne A (2006) Thermoplastic starch-waxy maize starch nanocrystals nanocomposites. *Biomacromol* 7:531–539
- Angles MN, Dufresne A (2000) Plasticized starch/tunicin whiskers nanocomposites. 1. Structural analysis. *Macromol* 33:8344–8353
- Angles MN, Dufresne A (2001) Plasticized starch/tunicin whiskers nanocomposite materials. 2. Mechanical behavior. *Macromol* 34:2921–2931
- Azizi Samir MAS, Alloin F, Dufresne A (2005) Review of recent research into cellulosic whiskers, their properties and their application in nanocomposite field. *Biomacromol* 6:612–626
- Beck-Candanedo S, Roman M, Gray DG (2005) Effect of reaction conditions on the properties and behavior of wood cellulose nanocrystal suspensions. *Biomacromol* 6:1048–1054
- Bondeson D, Mathew A, Oksman K (2006) Optimization of the isolation of nanocrystals from microcrystalline cellulose by acid hydrolysis. *Cellulose* 13:171–180
- Cao X, Dong H, Li CM (2007) New nanocomposite materials reinforced with flax cellulose nanocrystals in waterborne polyurethane. *Biomacromol* 8:899–904
- Carvalho AJF, Job AE, Alves N, Curvelo AAS, Gandini A (2003) Thermoplastic starch/natural rubber blends. *Carbohydr Polym* 53:95–99
- Chazeau L, Cavaille JY, Perez J (2000) Plasticized PVC reinforced with cellulose whiskers. II. Plastic behavior. *J Polym Sci B Polym Phys* 38:383–392
- Choi Y, Simonsen J (2006) Cellulose nanocrystal-filled carboxymethyl cellulose nanocomposites. *J Nanosci Nanotechnol* 6:633–639
- Choi EJ, Kim CH, Park JK (1999) Structure–property relationship in PCL/starch blend compatibilized with starch-g-PCL copolymer. *J Polym Sci B Polym Phys* 37:2430–2438
- Dufresne A, Kellerhals MB, Witholt B (1999) Transcrystallization in Mcl-PHAs/cellulose whiskers composites. *Macromol* 32:7396–7401
- Eichhorn SJ, Dufresne A, Aranguren M, Marcovich NE, Capadona JR, Rowan SJ, Weder C, Thielemans W, Roman M, Renneckar S, Gindl W, Veigel S, Keckes J, Yano H, Abe K, Nogi M, Nakagaito AN, Mangalam A, Simonsen J, Benight AS, Bismarck A, Berglund LA, Peijs T (2010) Review: current international research into cellulose nanofibres and nanocomposites. *J Mater Sci* 45:1–33
- Gaudin S, Lourdin D, Forssell PM, Colonna P (2000) Antiplasticization and oxygen permeability of starch–sorbitol films. *Carbohydr Polym* 43:33–37
- Gopalan Nair K, Dufresne A (2003) Crab shell chitin whisker reinforced natural rubber nanocomposites. 2. Mechanical behavior. *Biomacromol* 4:666–674
- Grunert M, Winter WT (2002) Nanocomposites of cellulose acetate butyrate reinforced with cellulose nanocrystals. *J Polym Environ* 10:27–30
- Huang M, Yu J, Ma X (2006) High mechanical performance MMT-urea and formamide-plasticized thermoplastic cornstarch biodegradable nanocomposites. *Carbohydr Polym* 63:393–399
- Karande VS, Mhaske ST, Bharimalla AK, Hadge GB, Vigneshwaran N (2013) Evaluation of two-stage process (refining and homogenization) for nanofibrillation of cotton fibers. *Polym Eng Sci* 53:1590–1597
- Kvien I, Oksman K (2007) Orientation of cellulose nanowhiskers in polyvinyl alcohol. *Appl Phys A* 87:641–643
- Kvien I, Sugiyama J, Votrubec M, Oksman K (2007) Characterization of starch based nanocomposites. *J Mater Sci* 42:8163–8171
- Ljungberg N, Bonini C, Bortolussi F, Boisson C, Heux L, Cavaille JY (2005) New nanocomposite materials reinforced with cellulose whiskers in atactic polypropylene: effect of surface and dispersion characteristics. *Biomacromol* 6:2732–2739
- Lu Y, Weng L, Zhang L (2004) Morphology and properties of soy protein isolate thermoplastics reinforced with chitin whiskers. *Biomacromol* 5:1046–1051
- Lu Y, Weng L, Cao X (2006) Morphological, thermal and mechanical properties of ramie crystallites—reinforced plasticized starch biocomposites. *Carbohydr Polym* 63:198–204
- Nishino T, Matsuda I, Hirao K (2004) All-cellulose composite. *Macromol* 37:7683–7687

- Petersson L, Kvien I, Oksman K (2007) Structure and thermal properties of poly (lactic acid)/cellulose whiskers nanocomposite materials. *Compos Sci Technol* 67:2535–2544
- Pu Y, Zhang J, Elder T, Deng Y, Gatenholm P, Ragauskas AJ (2007) Investigation into nanocellulosics versus acacia reinforced acrylic films. *Compos B Eng* 38:360–366
- Rane LR, Savadekar NR, Kadam PG, Mhaske ST (2014) Preparation and characterization of K-carrageenan/nanosilica biocomposite film. *J Mater* 2014:1–8
- Sanchez-Garcia MD, Lagaron JM (2010) On the use of plant cellulose nanowhiskers to enhance the barrier properties of polylactic acid. *Cellulose* 17:987–1004
- Savadekar NR, Mhaske ST (2012) Synthesis of nano cellulose fibers and effect on thermoplastics starch based films. *Carbohydr Polym* 89:146–151
- Savadekar NR, Kadam PG, Mhaske ST (2013) Studied on the effect of nano-alumina on the performance properties of poly(butylenes adipate-co-terephthalate) composite films. *J Thermoplast Compos Mater*. doi:[10.1177/0892705713513292](https://doi.org/10.1177/0892705713513292)
- Shimazaki Y, Miyazaki Y, Takezawa Y, Nogi M, Abe K, Ifuku S, Yano H (2007) Excellent thermal conductivity of transparent cellulose nanofiber/epoxy resin nanocomposites. *Biomacromol* 8:2976–2978
- Sorrentino A, Gorrasi G, Vittoria V (2007) Potential perspectives of bio-nanocomposites for food packaging applications. *Trends Food Sci Tech* 18:84–95
- Van Soest JGG, Benes K, De Wit D, Vliegthart JFG (1996) The influence of starch molecular mass on the properties of extruded thermoplastic starch. *Polymer* 37:3543–3552
- Wongpanit P, Sanchavanakit N, Pavasant P, Bunaprasert T, Tabata Y, Rujiravanit R (2007) Preparation and characterization of chitin whisker-reinforced silk fibroin nanocomposite sponges. *Eur Polym J* 43:4123–4135
- Zhang J, Elder TJ, Pu Y, Ragauskas AJ (2007) Facile synthesis of spherical cellulose nanoparticles. *Carbohydr Polym* 69:607–611